Effects of Truck Tire Contact Pressure Distribution on the Design of Flexible Pavements: A Three-Dimensional Finite Element Approach

HSIEN H. CHEN, KURT M. MARSHEK, AND CHHOTE L. SARAF

The objective of the study reported in this paper was to investigate the effect of high inflation pressure and heavy axle load on asphalt-concrete pavement performance by using a three-dimensional finite element model instead of an elastic layer model, which is commonly used for pavement design. The flexible pavement finite element analysis was conducted with both an experimental nonuniform pressure model and a uniform pressure model as input to the program TEXGAP–3D. The results show that *(a)* the uniform pressure model overestimated the increase in tensile strain at the bottom of the surface for overinflated tires and underestimated the increase in tensile strain at the bottom of the surface for overloaded tires, *(b)* both high inflation pressure and heavy load caused a high increase in tensile strain at the bottom of the surface and a significant reduction of the pavement fatigue damage life, and *(c)* the axle load (not the inflation pressure) had a major influence on the subgrade rutting life.

A previous investigation *(1)*, which used a nonuniform concentric circular pressure model, has presented results that show the effect of high inflation pressures and heavy loads on the critical tensile strain at the bottom of the surface course and the compressive strain at the top of the subgrade. This model was obtained by dividing the experimental tire-pavement contact pressure distribution (along the tire contact width at the center of the tire imprint) into 14 different pressure regions. The pressure in each region was averaged and the radial distance was adjusted so that the total load from the nonuniform concentric circular pressure model was equal in magnitude to the tire axle load. However, experimental results show that the shoulder regions of a truck tire produce two strips of high pressure that can dominate the whole contact pressure distribution. Compared with the experimental tire contact pressure distribution, neither the uniform pressure model nor the nonuniform concentric circular pressure model appears appropriate as input for a pavement stress analysis. Note that the uniform pressure model assumed the contact pressure to be uniform over the circular (or square) imprint area and equal in magnitude to the tire inflation pressure.

The main objective of this paper is to investigate the effects of high inflation pressure and heavy load on stress on and damage to asphalt-concrete pavement by using a three-dimensional finite element model (i.e., experimental tire-pavement contact pressure distribution) instead of the nonuniform circular pressure model.

There are several general-purpose finite element computer programs available that can be used to analyze pavement performance. For the three-dimensional contact pressure model, the computer program TEXGAP–3D was selected in this study to predict the performance of flexible pavements under various inflation pressures and truck tire axle loads.

H. H. Chen and K. M. Marshek, Mechanical Engineering Department, The University of Texas at Austin, Austin, Tex. 78712. C. L. Saraf, Center for Transportation Research, The University of Texas at Austin, Austin, Tex. 78712.

DESCRIPTION OF PROGRAM TEXGAP–3D

The TEXGAP–3D (Texas Grain Analysis Program) is a linear elastic, static, finite element code for the analysis of a three-dimensional continuum structure and as such is not a general-purpose code because it does not contain other element types (e.g., beam, plate, and shell elements). The element library includes quadratic, isoparametic 20-node bricks; 15-node triangular prisms; and 10-node tetrahedrons. Material models include isotropic, orthotropic, and anisotropic. Permissible loadings and boundary conditions include pressure and traction on a surface, sliding and clamped surfaces, and prescribed nodal point forces or displacements.

PAVEMENT MODEL

The pavement selected for analysis is typical of that used on Texas farm-to-market roads and the behavior of the pavement structure is assumed to be linear elastic and homogeneous. The modulus of elasticity, Poisson's ratio, and layer thickness of each layer are as follows:

Surface	
Thickness	1.5, 2.0, 3.0, and 4.0 in.
Surface modulus	400 ksi
Poisson's ratio	0.35
Base	
Thickness	8 in.
Base modulus	60 ksi
Poisson's ratio	0.40
Subgrade	
Thickness	169 in.
Subgrade modulus	6 ksi
Poisson's ratio	0.45

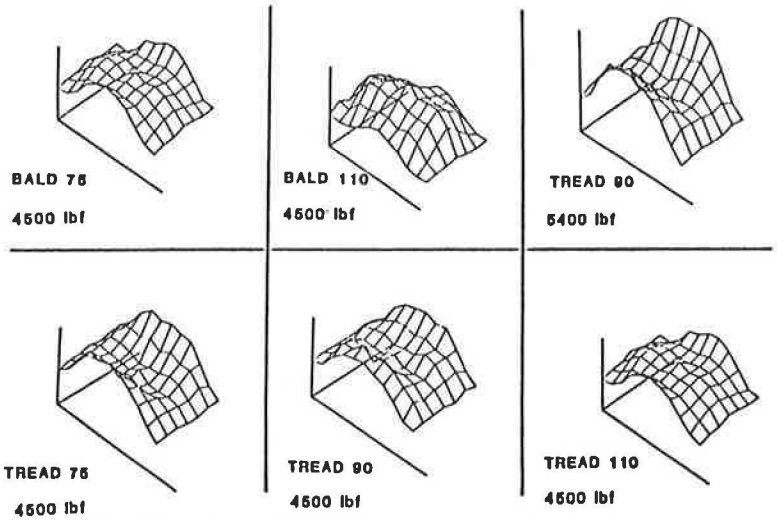

FIGURE 1 Experimental tire contact pressure distributions for various inflation pressures and axle loads.

PRESSURE DISTRIBUTION MODEL FOR TEXGAP–3D

The three-dimensional experimental truck tire contact pressure distributions for various tire inflation pressures (75, 90, and 110 psi) and axle loads (4,500 and 5,400 lbf) are shown in Figure 1. The pressure distribution model for an inflation pressure of 75 psi and an axle load of 4,500 lbf is given in Table 1. The pressure distributions input to TEXGAP–3D for the six cases studied in this paper are given elsewhere *(1)*. Because the contact pressure distributions are quite symmetric along the tire centerline, only one-quarter of the tire-pavement interaction was analyzed to minimize computer costs. The three-dimensional finite element model ($9 \times 6 \times 4$) consists of 216 solid brick elements. The element size was smallest within the contact pressure region as shown in the lower left corner of Figure 2. The pressure loading consists of 6×3 elements. Each element corresponds to an individual uniform contact pressure within the corresponding cell region. The bottom of the subgrade was assumed to be rigid.

EFFECT OF TIRE PRESSURE ON TENSILE STRAIN AT THE BOTTOM OF THE SURFACE

To demonstrate the accuracy of the TEXGAP–3D finite element model, results were compared with those of the layer program ELSYM5 for a uniform circular pressure model. Figure 3 shows the comparison of the three-dimensional uniform pressure model TEXGAP–3D and the uniform circular pressure model ELSYM5 for tensile strain at the bottom of the surface with various surface thicknesses (note that U designates uniform pressure model employing TEXGAP–3D and L designates the results from layer program ELSYM5). There is a close correspondence between the results from the two models. The increase of inflation pressure from 75 to 110 psi results in an approximate 102-microstrain (1 microstrain = 1×10^{-6} in./in.) increase at the bottom of a 1.5-in.-thick surface pavement. For the thicker surface pavements, the effect of the tire-pavement contact pressure distribution on surface tensile strain becomes less significant.

Figure 4 shows a comparison of the experimental non-

TABLE 1 EXPERIMENTAL TIRE CONTACT PRESSURE DISTRIBUTION MODEL FOR TEXGAP–3D

Along-Tire Contact Length (in.)	Along-Tire Contact Width (in.)											
	0	0.43	1.08	1.61	2.15	3.23	4.2	5.16	6.24	6.78	7.31	8.0	8.4
0	46	59	50	33	58	63	58	62	16	67	73	52	
1.47	112	96	64	35	65	59	52	68	44	59	98	124	
2.83	134	98	98	0	45	50	46	55	15	92	98	138	
4.25	133	101	71	36	63	60	55	55	17	87	97	125	
5.67	113	100	74	34	60	49	48	74	46	56	94	111	
7.09	66	62	59	17	54	34	50	58	25	65	66	57	
8.5													

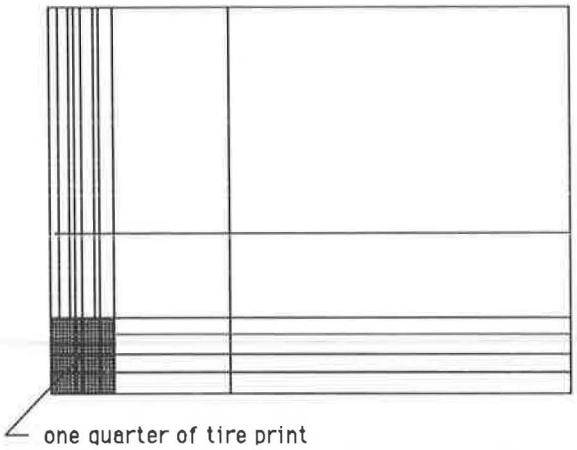

FIGURE 2 Grid formulation at the surface of the asphalt-concrete pavement (5 ft long by 5 ft wide).

uniform pressure model (T7545. T11045) and the uniform pressure model (U7545, U11045) for tensile strain at the bottom of the surface with various surface thicknesses (T designates the treaded-tire experimental contact pressure model). With a 47 percent increase in the inflation pressure (for the same axle load), the uniform pressure model predicts a 62 percent increase in the surface tensile strain at the bottom of the 1.5-in.-thick pavement, whereas the experimental model yields a 33 percent increase in the surface tensile strain. The uniform pressure model overestimates the reduction of contact area with an increased inflation pressure (for the same axle load) from 75 to 110 psi. For example, with the 47 percent increase in tire inflation pressure, the uniform pressure model will produce a 32 percent decrease in contact area compared with a measured 9 percent decrease in truck tire gross contact area.

For the 2-in.-thick surface pavement, the effect of increased

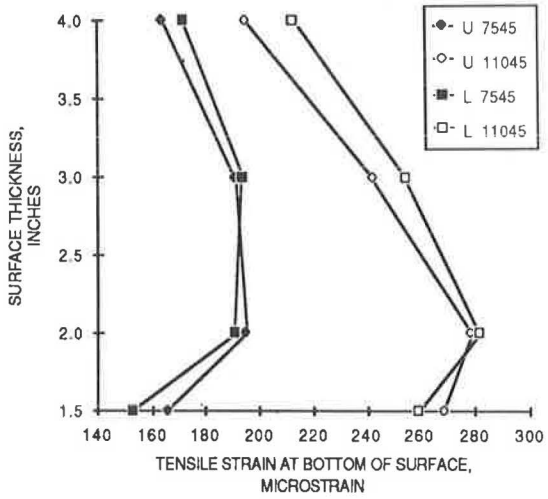

FIGURE 3 Effect of pressure distribution model on critical tensile strain at the bottom of the surface. U and L, respectively, represent the analysis obtained using TEXGAP–3D and ELSYM5, and the values 7545 and 11045 are for a tire loaded at 4,500 lbf with inflation pressures of 75 and 110 psi, respectively.

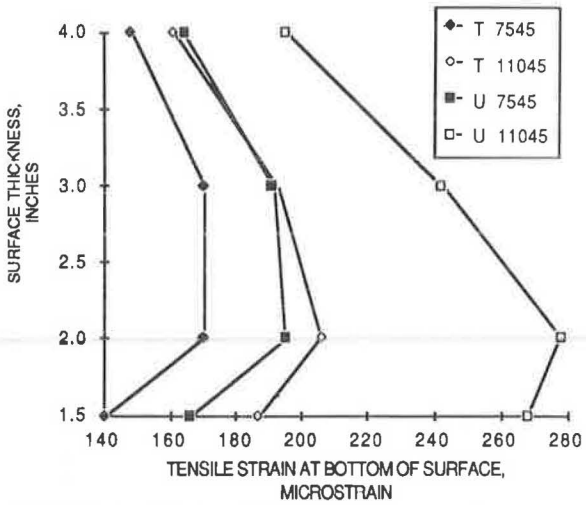

FIGURE 4 Effect of inflation pressure on the critical tensile strain at the bottom of the surface. T designates a treaded tire with a nonuniform (experimental) pressure model, and U designates a uniform pressure model. The values 7545 and 11045 represent, respectively, a tire loaded at 4,500 lbf with inflation pressures of 75 and 110 psi.

inflation pressure on the surface tensile strain along the tire transverse direction is shown in Figure 5. At a distance of 6 in. from the tire centerline, inflation pressure will have no significant effect on surface tensile strain.

EFFECT OF AXLE LOAD ON TENSILE STRAIN AT THE BOTTOM OF THE SURFACE

Figure 6 shows the effect of tire axle load on critical tensile strain for surface thickness of from 1.5 to 4.0 in. for both the nonuniform experimental pressure model and the uniform pres-

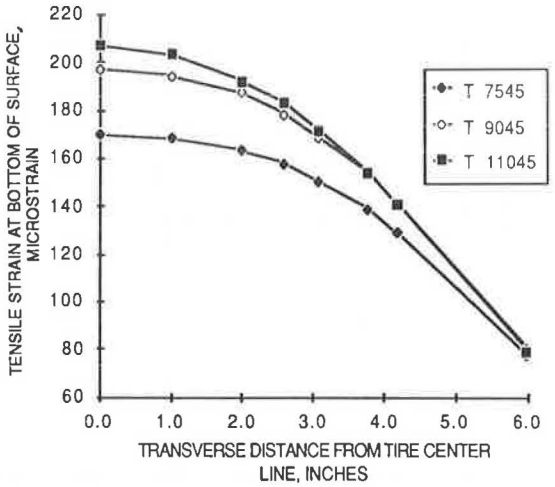

FIGURE 5 Effect of inflation pressure on the tensile strain contour at the bottom of a 2-in.-thick surface pavement. T designates a treaded tire; the values 7545, 9045, and 11045 represent, respectively, a tire loaded at 4,500 lbf with inflation pressures of 75, 90, and 110 psi.

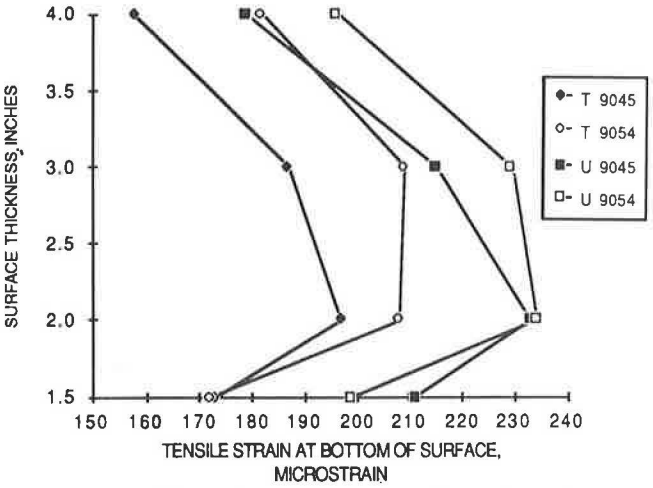

FIGURE 6 Effect of axle load on tensile strain at the bottom of the surface. T designates a treaded tire with nonuniform (experimental) pressure model, and U designates a uniform pressure model. The values 9045 and 9054 represent, respectively, a 90-psi tire inflation pressure with loads of 4,500 and 5,400 lbf.

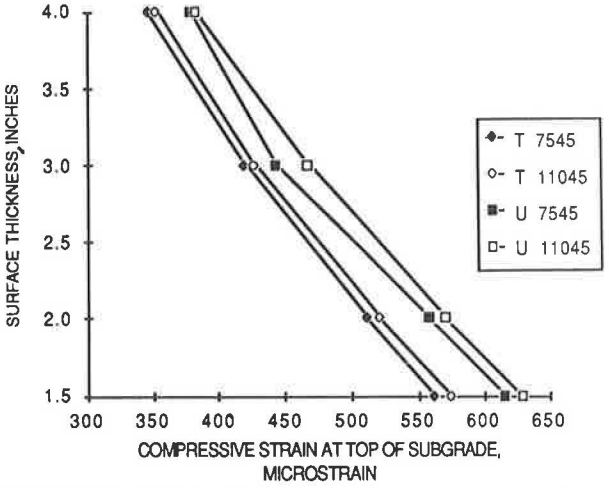

FIGURE 8 Effect of inflation pressure on compressive strain at the top of the subgrade. T designates a treaded tire with a nonuniform (experimental) pressure model, and U designates a uniform pressure model. The values 7545 and 11045 represent, respectively, a tire loaded at 4,500 lbf with inflation pressures of 75 and 110 psi.

sure model. The results from the uniform pressure model are conservative in comparison with those of the experimental model for various surface thicknesses. As anticipated, the overloaded tire consistently produces the highest strains. For a 4.0-in.-thick surface pavement and a 20 percent increase in the axle load (for the same tire inflation pressure), the uniform pressure model results in a 10 percent increase in the surface tensile strain compared with a 15 percent increase for the experimental pressure model. The uniform pressure model overestimates the increase of the contact area and therefore produces a smaller increase in surface tensile strain.

Figure 7 shows the tensile strain developed at the bottom of the 2-in.-thick surface course by the application of a 4,500-lbf load and a 5,400-lbf load (20 percent overload) to the treaded tire at the 90-psi–rated inflation pressure. The overloaded tire consistently produces a higher tensile strain even at a distance of 6.0 in. from the tire centerline.

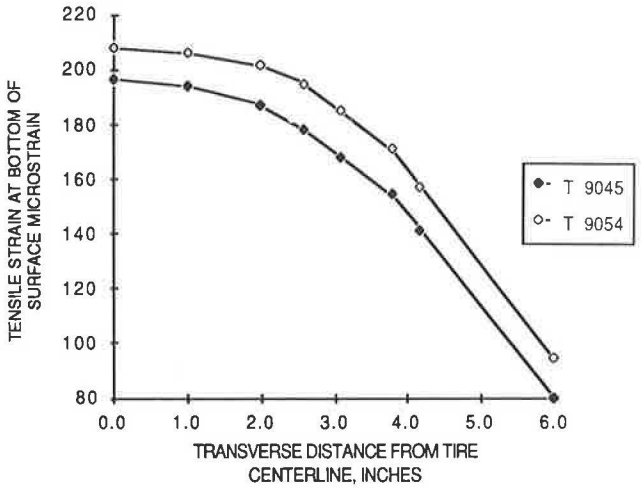

FIGURE 7 Effect of axle load on tensile strain at the bottom of a 2-in.-thick surface pavement. T designates a treaded tire, and the values 9045 and 9054 represent, respectively, a 90-psi tire inflation pressure with loads of 4,500 and 5,400 lbf.

EFFECT OF TIRE PRESSURE ON SUBGRADE COMPRESSIVE STRAIN

Figure 8 shows that a 47 percent increase in inflation pressure (for the same axle load) produces less than a 2 percent increase in the compressive strain developed at the top of the subgrade for both the uniform pressure model and the nonuniform experimental pressure model. The uniform pressure model consistently overestimates the subgrade compressive strain except for thick surface pavements.

EFFECT OF AXLE LOAD ON SUBGRADE COMPRESSIVE STRAIN

Figure 9 shows that the axle load has a significant effect on the compressive strains at the top of the subgrade for both the uniform pressure model and the nonuniform pressure model. The figure shows that a 20 percent increase in axle load (for the same inflation pressure) produces approximately a 20 percent increase in the critical subgrade compressive strain for both models. However, the uniform pressure model consistently overestimated the subgrade compressive strain (compared with the strain obtained by the nonuniform pressure model) for the range of surface thicknesses shown.

PAVEMENT DAMAGE

The two primary pavement distress conditions addressed in this analysis are fatigue and rutting. Fatigue cracks may develop if

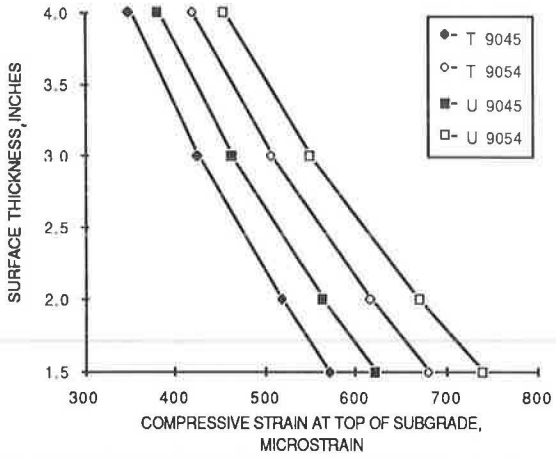

FIGURE 9 Effect of axle load on compressive strain at the top of the subgrade. T designates a treaded tire with a nonuniform (experimental) pressure model, and U designates a uniform pressure model. The values 9045 and 9054 represent, respectiveiy, a 90-psi tire inflation pressure with loads of 4,500 and 5,400 lbf.

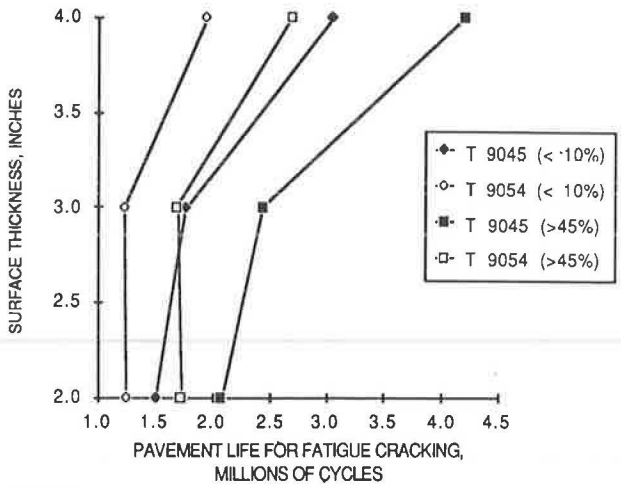

FIGURE 11 Effect of axle load on pavement fatigue damage life. T designates a treaded tire, and the values 9045 and 9054 represent, respectively, a 90-psi tire inflation pressure with loads of 4,500 and 5,400 lbf.

the tensile strain at the bottom of the asphalt layer is excessive. Rutting, the permanent deformation that leads to loss of surface shape, may occur if the compressive strain at the top of the subgrade is excessive.

FATIGUE-CRACKING DAMAGE

Flexible pavement fatigue is manifested by the appearance of alligator cracking in the wheelpaths and is caused by excessive tensile stresses and strains at the bottom of the asphalt-concrete surface layer. The tensile strains that have been computed using TEXGAP–3D at the bottom of the asphalt-concrete surface are used to approximate the number of 18-kip axle load applications until Class 2 cracking occurs. Class 2 cracking is defined as the appearance of alligator cracking. Class 3 cracking is defined as the progression of alligator cracking to severe spalling. A pavement surface that has Class 2 cracking is assumed to have failed in fatigue.

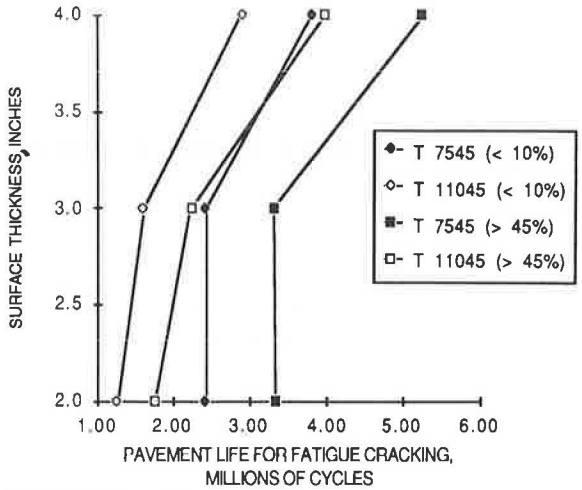

FIGURE 10 Effect of inflation pressure on pavement fatigue damage life. T designates a treaded tire, and the values 7545 and 11045 represent, respectively, a tire loaded at 4,500 lbf with inflation pressures of 75 and 110 psi.

Predictions of the number of loads (N_f) necessary to cause fatigue failure have been developed in the literature. Such predictions are based on laboratory tests, with little correlation to field experience to account for the relaxation times between traffic loads and the resulting differences in crack propagation rates. A literature survey showed that the number of wheel loads required to initiate fatigue distress is on the order of 13 to 18 times that predicted by constant stress laboratory tests *(2)*.

A field fatigue distress model was developed by Finn et al. *(2)* for two levels of cracking: *(a)* cracking less than or equal to 10 percent of the wheelpath area and *(b)* cracking equal to or greater than 45 percent of the wheelpath area. These equations are

$$\log N_f (\leq 10\%) = 15.947 - 3.291 \log \varepsilon_t - 0.854 \log E^* \quad (1)$$

$$\log N_f (\geq 45\%) = 16.086 - 3.291 \log \varepsilon_t - 0.854 \log E^* \quad (2)$$

where

N_f = the number of loads of constant stress necessary to cause fatigue cracking,
ε_t = the initial tensile microstrain at the bottom of the surface, and
E^* = the complex modulus of the asphalt-concrete surface (ksi).

The number of loads of constant stress necessary to cause fatigue cracking can be obtained by substituting the computed tensile strain from finite element program TEXGAP–3D into Equations 1 and 2 for either the 10 percent cracking model or the 45 percent cracking model. Figure 10 shows the effect of

TABLE 2 TENSILE STRAIN AT THE BOTTOM OF THE SURFACE AND CORRESPONDING FATIGUE LIFE FOR VARIOUS SURFACE THICKNESSES, INFLATION PRESSURES, AND AXLE LOADS

	Tensile Strain at Bottom of Surface (10^{-1} in./in.) for Surface Thickness of (in.)			10% Fatigue-Cracking Model (million cycles) for Surface Thickness of (in.)			45% Fatigue-Cracking Model (million cycles) for Surface Thickness of (in.)		
	2.0	3.0	4.0	2.0	3.0	4.0	2.0	3.0	4.0
T7545	170.0	170.4	148.1	2.42	2.40	3.82	3.34	3.31	5.26
T11045	206.5	192.3	161	1.27	1.62	2.90	1.76	2.23	3.99
T9045	196.5	187	158.4	1.51	1.77	3.06	2.07	2.44	4.21
T9054	208	208.9	181.6	1.25	1.23	1.95	1.72	1.69	2.69
U7545	194.6	191.1	163.8	1.55	1.65	2.74	2.14	2.27	3.77
U11045	277.8	242	194.5	0.48	0.76	1.56	0.66	1.04	2.14
U9045	232.6	214.8	178.6	0.864	1.12	2.06	1.19	1.55	2.84
U9054	233.6	228.8	196.5	0.85	0.91	1.50	1.17	1.26	2.07

Note: T designates a treaded tire, with a nonuniform (experimental) pressure model, and U designates a uniform model. The last two digits (45 and 54) stand for 4,500 lbf and 5,400 lbf, respectively, and the numbers 75, 90, and 110 represent inflation pressures of 75, 90, and 110 psi, respectively.

increasing tire inflation pressure on fatigue damage life for various surface thicknesses. Pavement life improves with thicker pavement. For the 2-in.-thick surface pavement, a 47 percent increase in the tire inflation pressure (for the same axle load) results in a 33 percent increase in the surface tensile strain and therefore in a 48 percent reduction of pavement life for the 10 percent fatigue-cracking model and the 45 percent fatigue-cracking model. Figure 11 shows the effect of truck tire overload on the pavement fatigue life for various surface thicknesses (2 to 4 in.). For a 4-in. surface pavement, a 20 percent increase in axle load (for the same tire inflation pressure) will cause a 36 percent reduction in pavement life for both fatigue-cracking models. The tensile strains at the bottom of the surface and the corresponding number of constant stress cycles (N_f) necessary to cause either 10 or 45 percent fatigue cracking are given in Table 2 for various surface thicknesses, inflation pressures, and axle loads.

RUTTING

Rutting in the wheelpaths results from high compressive strains and permanent deformation in one or more pavement layers, influenced by truck tire axle load, layer properties, environment, and number of traffic loadings. Analysis of the AASHO Road Test showed that lateral movement of material in the subbase accounted for most of the rutting observed *(3)*.

To minimize surface rutting, Shell Company engineers used results from the AASHO Road Test to develop a compressive strain criteria equation *(4)*:

$$W_{18} = 6.15 \times 10^{17} (1/\varepsilon_c)^{4.0} \quad (3)$$

where ε_c is the compressive microstrain at the top of the subgrade, and W_{18} is the number of weighted 18-kip axle loads before excessive permanent deformation.

Figure 12 shows the effect of increasing the axle load on the subgrade rutting damage life for various surface thicknesses. A 20 percent increase in axle load (for the same inflation pressure) will result in a 19 percent increase in subgrade compressive strain and a 50 percent reduction in pavement life. The subgrade compressive strains and the corresponding rutting life are given in Table 3 for various surface thicknesses, inflation pressures, and tire axle loads.

CONCLUDING REMARKS

The effects of high inflation pressure and heavy load on asphalt-concrete pavement stresses, strains, and the corresponding pavement damage life were analyzed using the three-dimensional finite element tire-pavement contact pressure model rather than the uniform circular pressure model or the nonuniform concentric circular pressure model.

The computation time for a single run on TEXGAP–3D (216 brick elements) was approximately 18 min, corresponding to $80 per case, compared with a 2.5-sec execution time using the layer program ELSYM5.

Table 4 gives a comparison of the three-dimensional finite element model (uniform or nonuniform pressure distribution) and ELSYM5. On the basis of the limited number of tire contact pressure distributions and pavements studied, it can be

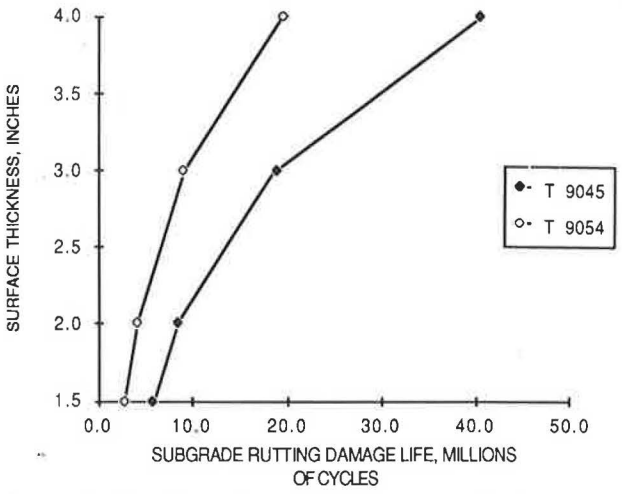

FIGURE 12 Effect of axle load on pavement subgrade rutting damage life. T designates a treaded tire, and the values 9045 and 9054 represent, respectively, a 90-psi tire inflation pressure with loads of 4,500 and 5,400 lbf.

TABLE 3 COMPRESSIVE STRAIN AT THE TOP OF THE SUBGRADE AND THE CORRESPONDING PAVEMENT DAMAGE LIFE FOR VARIOUS SURFACE THICKNESSES, INFLATION PRESSURES, AND AXLE LOADS

	Compressive Strain at Top of Subgrade ($\times 10^{-6}$ in./in.) for Surface Thickness of (in.)				Million Load Cycles Before Excessive Deformation (rutting) for Surface Thickness of (in.)			
	1.5	2.0	3.0	4.0	1.5	2.0	3.0	4.0
T7545	562.8	510.8	419.6	347.2	6.13	9.03	19.8	42.3
T11045	575.3	521.4	427.2	352.6	5.61	8.32	18.5	39.8
T9045	571	518	424.7	351	5.78	8.54	18.9	40.5
T9054	681	618.3	508	420.4	2.86	4.21	9.23	19.7

TABLE 4 COMPARISON OF VARIOUS MODELS FOR TENSILE STRAIN AND SUBGRADE COMPRESSIVE STRAIN

	47% Increase in Tire Inflation Pressure			20% Increase in Truck Tire Axle Load		
	Nonuniform	Uniform	ELSYM5	Nonuniform	Uniform	ELSYM5
Tensile strain at bottom of surface (% increase)	33	62	69	15	10	8
Subgrade compressive strain (% increase)	2	2	5	19	19	17

concluded that the uniform pressure model overestimates the tensile strain at the bottom of the surface for either underinflated or overinflated tires. The uniform pressure model will predict a higher percentage increase in tensile strain than will the nonuniform experimental pressure model. However, with the same percentage increase in truck tire axle load, the uniform pressure model will underestimate the percentage increase in the surface tensile strain.

Inflation pressure will have less than a 2 percent effect on the compressive strains at the top of the subgrade for either the uniform pressure model or the nonuniform pressure model. Therefore inflation pressure is an insignificant factor in subgrade rutting.

Axle load has a significant effect on subgrade compressive strain and corresponding subgrade rutting life. A 20 percent increase in the axle load results in a 19 percent increase in the subgrade compressive strain and an approximately 50 percent reduction of pavement life.

ACKNOWLEDGMENTS

The authors are pleased to acknowledge the combined efforts and support of the Center for Transportation Research and the Mechanical Engineering Department at the University of Texas at Austin and the Texas State Department of Highways and Public Transportation, in cooperation with the Federal Highway Administration, U.S. Department of Transportation.

REFERENCES

1. K. M. Marshek, W. R. Hudson, H. H. Chen, C. Saraf, and R. B. Connell. *Effect of Truck Tire Inflation Pressure and Axle Load on Pavement Performance.* Research Report 386–2F. Center for Transportation Research, The University of Texas at Austin, 1985.
2. F. Finn et al. The Use of Distress Prediction Subsystems for the Design of Pavement Structures. *Proc., 4th International Conference on the Structural Design of Asphalt Pavements,* University of Michigan, Ann Arbor, Aug. 1977.
3. *Special Report 61E: The AASHO Road Test: Report 5—Pavement Research.* HRB, National Research Council, Washington, D.C., 1962.
4. *Shell Pavement Design Manual.* Shell International Petroleum Company Limited, London, England, 1978.

Publication of this paper sponsored by Committee on Flexible Pavements.